Journal of Hydrology 628 (2024) 130508

Contents lists available at ScienceDirect

Journal of Hydrology

journal homepage: www.elsevier.com/locate/jhydrol

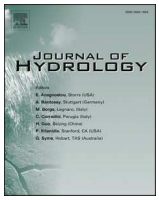

Research papers

Interpreting floodplain heterogeneity: Using field data to understand unsupervised floodplain classifications

Emily Iskin *, Ellen Wohl

Department of Geosciences, Colorado State University, Fort Collins, CO, United States

ARTICLE INFO

This manuscript was handled by Nandita Basu, Editor-in-Chief, with the assistance of Rebecca Logsdon Muenich, Associate Editor

Keywords:
Floodplains
Spatial heterogeneity
Remote sensing
Landscape ecology
Unsupervised classification
Interpretation

ABSTRACT

The dynamic environment of natural river floodplains creates spatial heterogeneity that influences floodplain functions. Diverse human activities have homogenized natural floodplains and reduced their functions across many river networks in the temperate latitudes. Consequently, quantification of floodplain heterogeneity is needed to understand patterns of spatial heterogeneity on diverse floodplains and to inform floodplain restoration. We use a novel approach of spatially connecting field and remotely sensed data in order to interpret the output of, and build upon, a previous unsupervised classification workflow. We apply the method to three rivers in the US Pacific Northwest and the Altamaha River in the southeastern US and compare our results to a previous study. We find that field classifications, relative topography, and NDVI are useful for interpreting results from the unsupervised classification workflow. The interpretations are visually interesting, but we propose that it is the heterogeneity within the groups that is vital to floodplain functioning. Natural floodplains in the Pacific Northwest and coastal Southeast have moderate to high evenness, moderate to high intermixing, and moderate aggregation; and aggregation and evenness similar to rivers in Colorado and Oklahoma, USA, but lower intermixing. We attribute lower intermixing at the Altamaha River to slower rates of lateral channel migration, and lower intermixing at the Hoh River to the different hydrologic and sediment regimes and less stable braided planform. The results show that the larger rivers in this study (Altamaha, Hoh, and Sol Duc Rivers) have spatial heterogeneity similar to beaver-modified and shortgrass prairie rivers in Colorado, whereas the more inland and smaller river (Lookout Creek) has spatial heterogeneity similar to the tallgrass prairie site (Sand Creek). From the results of an ad hoc sensitivity analysis, we suggest using the highest spatial resolution topographic data available, using aerial imagery/mosaics from the same sensor, and removing largest patch index from the suite of comparable indices. The metrics reveal similarities and differences between rivers in the United States, and indicate that discernable trends may arise from a meta study comparing heterogeneity from more rivers across the country.

1. Introduction

River corridors are dynamic environments in which channel movements, fluxes of materials, and other natural disturbances create and maintain spatial heterogeneity (e.g., Fetherston et al., 1995; Stanford et al., 2005; Collins et al., 2012). Spatial heterogeneity is an intrinsic property of floodplain ecosystems and strongly influences floodplain functions (e.g., Stoffers et al., 2022), including surface and subsurface transport and storage of water (Helton et al., 2014); fluxes of sediment; storage, transformation, and consumption of large wood, nutrients, and pollutants (e.g., Appling et al., 2014); availability of diverse habitats (Stanford et al., 2005); and resilience to natural disturbances such as floods, drought, and wildfire (Wohl et al., 2022; Lane et al., 2023). This heterogeneity can be observed in many aspects of floodplain form, e.g. topography, standing water features, large wood distribution, and vegetation communities, and can be quantified with remote sensing and landscape ecology (Iskin & Wohl, 2023).

Loss of natural floodplains and their functions because of dams, diversions, levees, disconnection, stabilization, agriculture, and urban development, leads to decreased resilience of these landscapes and increased risk of destruction to both natural and human habitats (Knox et al., 2022b). Human-led alteration and management of river corridors is increasing (Knox et al., 2022a; Morrison et al., 2023), and is linked to lower spatial heterogeneity and functionality (Kuiper et al., 2014;

* Corresponding author.
E-mail address: Emily.Iskin@colostate.edu (E. Iskin).

https://doi.org/10.1016/j.jhydrol.2023.130508

Available online 21 November 2023

Samaritani et al., 2011; Schindler et al., 2016; Wohl & Iskin, 2019). Because spatial heterogeneity of floodplain form is linked to ecosystems functions, quantifying heterogeneity can provide insight into the form and associated functions of natural river corridors. A detailed understanding of floodplain heterogeneity at multiple sites could inform future river corridor restoration.

1.1. Objectives

Floodplain heterogeneity has been quantified in different ways during the last two decades, including using field data, remote sensing, and modeling (Ward et al., 2002; Aguiar et al., 2009; Gostner et al., 2013; Hugue et al., 2016; Scown et al., 2015, 2016; Wohl & Iskin, 2019; Iskin & Wohl, 2023). This study builds directly on Iskin & Wohl's (2023) recent study that developed a remote sensing workflow using unsupervised classification to quantify different facets of floodplain heterogeneity in Colorado and Oklahoma. We use a novel approach to interpret unsupervised classes by mining the data layers used in the classification and relating them to field observations. We also expand the geographical range to include the Pacific Northwest and coastal Georgia and add higher-resolution layers to the workflow.

Our objectives are to interpret results from an unsupervised classification by (1) modifying the workflow from Iskin and Wohl (2023) by adding more precise data and (2) spatially connecting the classification

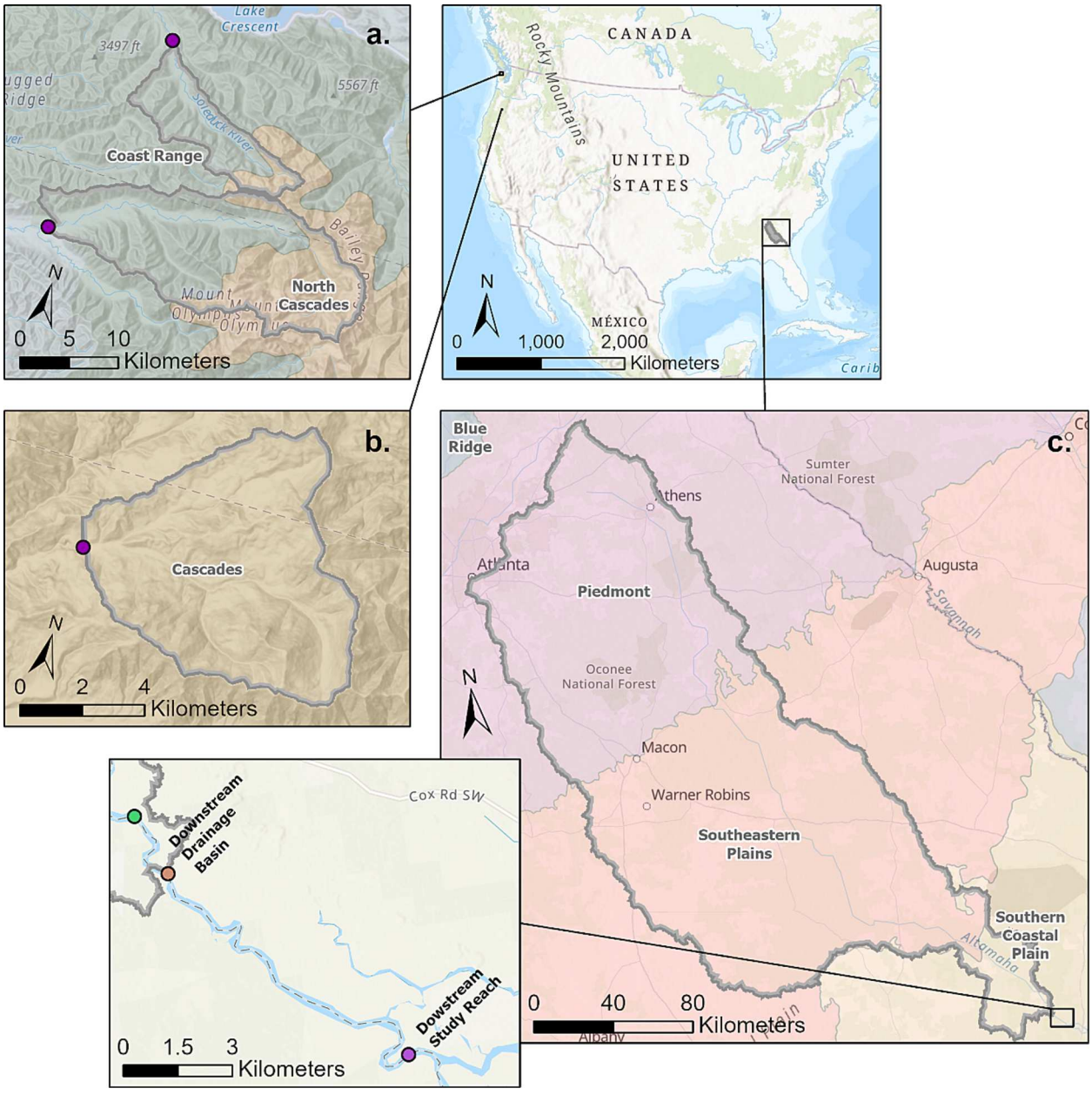

Fig. 1. Location map and drainage area maps of the field sites: a) the Sol Duc River (top) and the Hoh River (bottom), Washington; b) Lookout Creek, Oregon; and c) the Altamaha River, Georgia with detail inset. Map shows the drainage area boundaries upstream of the study reaches and the downstream-most point of each study reach (purple points) overlaid on the colored and labeled Level III Ecoregions, or areas with similar ecosystems (EPA, 2013). The drainage basin for the Altamaha River includes 2.4 km of the study reach and excludes 11.2 km of the study reach (downstream) because of limitations in StreamStats and proximity to the coastline (locations shown in the callout). (For interpretation of the references to colour in this figure legend, the reader is referred to the web version of this article.)

Table 1
Study area characteristics, where the "Study Reach" is the floodplain where field data were collected, and "Drainage Basin" is the basin delineated in StreamStats upstream of the downstream-most part of the study reach.

	Characteristic	Lookout Creek	Hoh River	Sol Duc River	Altamaha River [2]	Source
Study Reach	Level II Ecoregion of study reach	Western Cordillera	Marine West Coast Forest and Western Cordillera	Marine West Coast Forest and Western Cordillera	Mississippi Alluvial and Southeast USA Coastal Plains	EPA, 2013
	Level III Ecoregion of study reach	Cascades	Coast Range and North Cascades	Coast Range and North Cascades	Southern Coastal Plain	
	Underlying lithology of study reach	Undifferentiated tuffaceous sedimentary rocks, tuffs, and basalt with basalt and basaltic-andesite; Landslide and debris-flow deposits with coarse-detrital	Mesozoic-Tertiary marine rocks, undivided with graywacke, slate, and argillite	Younger glacial drift with fine- and coarse-detrital; Alluvium with silt and sand; and Mesozoic-Tertiary marine rocks, undivided with graywacke, slate, and argillite	Stream alluvium; Holocene Shoreline Complex - marsh and lagoonal facies; and Pamlico shoreline complex - marsh and lagoonal facies all with fine-detrital	Horton, 2017; Horton et al., 2017; USGS, 2022d
	Floodplain area (ha)	6.9	987.8	58.1	3,705.3	Field delineation
	Dates field data collected	7/6/2022 to 7/13/2022	7/7/2021 to 7/18/2021	7/6/2021 to 7/17/2021	10/19/2021	
Drainage Basin	Drainage area upstream of study reach (km^2)	53.6	323	101	36,500	USGS, 2022c, 2023a
	Mean basin annual precipitation (mm)	2,263.1	4,343.4	2,590.8	1,229.4 [3]	
	Mean basin elevation (m)	1,033	978	975	132	
	Mean basin slope from 30-m DEM	37 % [1]	56 %	52 %	5 % [4]	
Site Characteristics	Channel planform	Straight to Anastomosing	Braided to Anastomosing	Meandering to Straight	Meandering to Straight	Field observation
	Flow regime	Rain and snow	Rain and snow	Rain and snow	Rainfall dominated	
	Dominant vegetation	Conifer forest	Conifer rainforest	Conifer forest	Swamp forest	
	Confinement	Confined	Unconfined	Confined	Unconfined	
	Soil Type	Jimbo-Greenpeter-Manlywham complex, 0–15 % slopes; Aschoff-Kinney complex, 40–85 % slopes, south-facing; and Saturn clay loam, 0–5 % slopes	Isomesic valley bottom floodplain, river channel, and alluvial terraces, 0–15 % slopes	Mesic valley bottom floodplain, river channel, and alluvial terraces, 0–15 % slopes; Colluvial debris aprons, 15–60 % slopes	Swamp, 0–2 % slopes; Galestown fine sand, 0–2 % slopes; Satilla silt loam, 0–1 % slopes; Bladen loam and clay loam, 0–2 % slopes; Meggett loam, frequently flooded, 0–2 % slopes	NRCS, 2022a, 2022b, 2023

[1]Source topographic data not indicated in StreamStats, converted from slope degrees to slope percent.
[2]The drainage basin for the Altamaha River includes 2.4 km of the study reach and excludes 11.2 km of the study reach (downstream) because of limitations in StreamStats and proximity to coastline (an exclusion area).
[3]Basin average mean annual precipitation for 1971–2000 from PRISM
[4]From 10-m DEM

output to the field classes and soil core data. We also aim to (3) qualitatively compare our results from Washington, Oregon, and Georgia to the values of floodplain heterogeneity from Colorado and Oklahoma.

2. Study area

This study focuses on natural floodplains in the Pacific Northwest and Southeast regions of the United States (Fig. 1). The Hoh and Sol Duc Rivers are located in Olympic National Park in Washington and have adjacent watersheds (Fig. 1a). Lookout Creek runs through the HJ Andrews Experimental Forest near the town of McKenzie Bridge, Oregon (Fig. 1b). The study reach of the Altamaha River is located in coastal Georgia, but the watershed covers most of the State and originates in the Piedmont ecoregion (EPA, 2013). The sites intentionally span geographic, hydrologic, topographic, and ecologic conditions in order to capture some of the range of natural variability of river corridors in the continental U.S (Table 1).

3. Methods

Data were collected using field measurements and compilation of remote imagery (Table 3). The study areas were chosen based on geomorphic reaches with generally consistent planform and confinement. Field data were collected along 10 transects running across the floodplain perpendicular to the valley trend and spaced apart approximately 10 times the average channel width (Fig. 2). Because of lack of access and steep terrain in some areas, we only collected data along seven river-right transects at the Hoh River (Fig. 2). We encountered

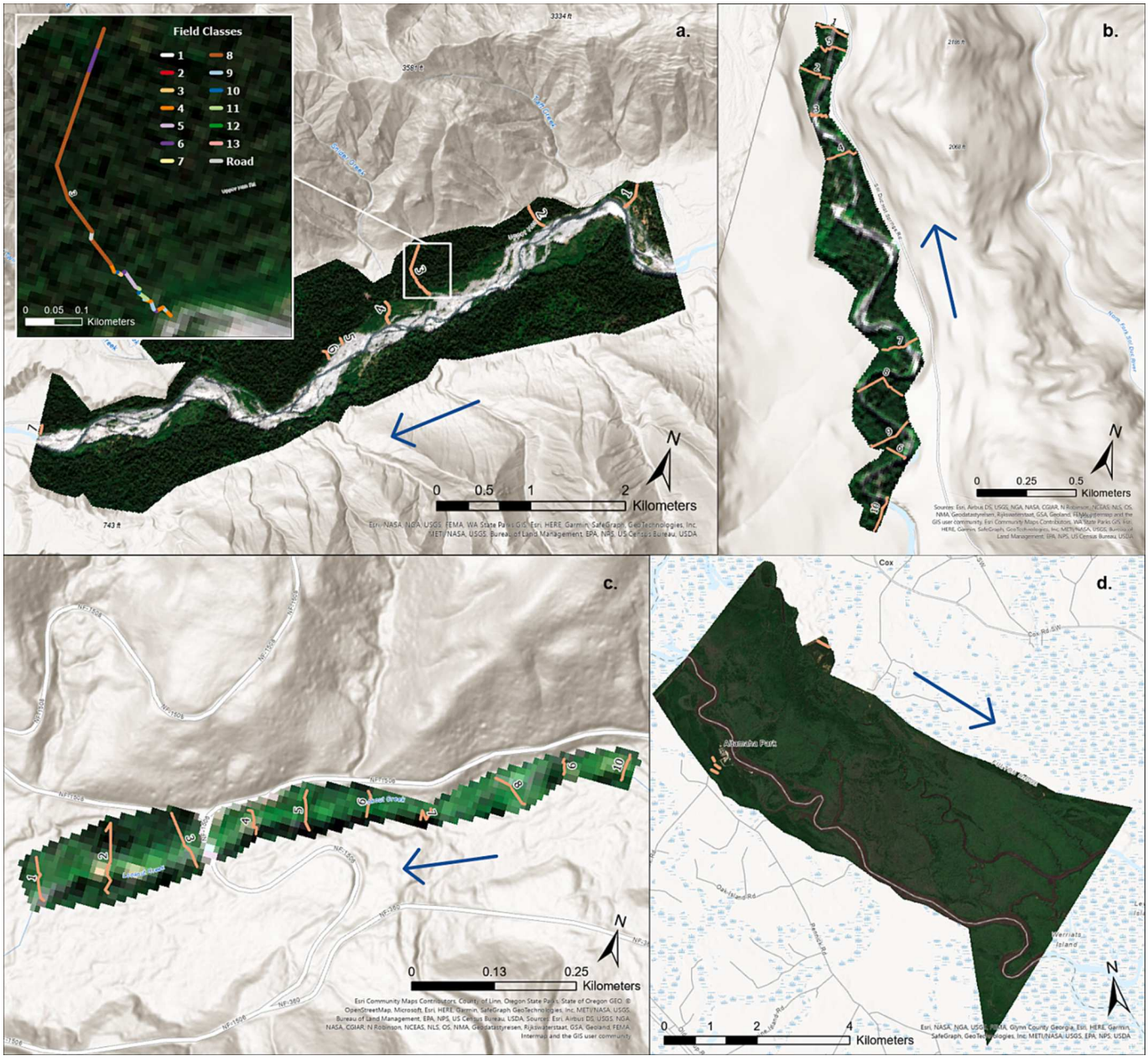

Fig. 2. Floodplain boundaries and field transects for a) the Hoh River, Washington with detail inset; b) the Sol Duc River, Washington; c) Lookout Creek, Oregon; and d) the Altamaha River, Georgia. Blue arrows indicate flow direction. The floodplain boundaries are shown with clipped Sentinel-2A mosaics and the labeled transects are shown in orange. The detail inset for the Hoh River shows a close up of Transect 3 and field classes delineated along that transect indicted by the different colors. The "transects" for the Altamaha River are not numbered and do not span the floodplain because of lack of access as described in the text. (For interpretation of the references to colour in this figure legend, the reader is referred to the web version of this article.)

unexpected high flows at the Altamaha River that almost completely inundated the floodplain and restricted access to areas near Altamaha Regional Park on river-right and along abandoned Seaboard Air Line Railroad Company infrastructure (Mcnally & Seaboard, 1896) starting on river-left and spanning the river, and therefore only collected data in these areas (Fig. 2). Along each transect qualitative habitat types, or "field classes," were mapped with handheld GPS based on observations of relative vegetation age and type, local topography, and fluvial features (Table 2) following the same techniques as Iskin and Wohl (2023). We differentiated 10 classes at the Sol Duc River in July 2021, 13 at the Hoh River in July 2021, and 13 at Lookout Creek in July 2022, all after seasonal peak flows. We differentiated 7 classes at the Altamaha River in October 2021.

Hand-driven soil cores were also collected along the transects (Fig. 3). Two cores per field class were collected at three depths where possible (approximately 0–30, 30–60, and 60–90 cm). In some cases, we could not physically core to the full 90 cm because of resistant layers such as cobbles and boulders. Core location, depth, and categorical moisture (dry, moist, saturated) were noted in the field. Soil cores were subsequently sent to Ward Laboratories in Kearney, Kansas for soil texture analysis. For the Hoh River, 48 of 52 submitted soil samples were suitable for lab analysis, 24 of 25 for the Sol Duc River, and 19 of 36 for Lookout Creek. No soil cores were collected at the Altamaha River because of flooded conditions. The field class delineations and soil core data are important for interpreting the results from the unsupervised classification.

Once the field work was complete, we proceeded to collect remote sensing data that coincides with the floodplains. Imagery used are Sentinel-2A raster mosaics from 2022 prepared in Google Earth Engine (Gorelick et al., 2017). Floodplain topography was constrained with

Table 2
Field class descriptions.

River	Class No.	Description
Hoh River	1	3 m high sediment deposit, fine sand to large cobbles, some bushy vegetation and dried grasses, old braid surface
	2	≤ to 10 cm DBH alders closely spaced, viny groundcover and moist soil
	3	40 cm DBH alders, 40–120 cm DBH conifers, bracken fern, abundant low groundcover, natural levee surface
	4	Undulating topo, 20–40 cm DBH alders, abundant bracken fern
	5	Waist high grasses, dry surface, drained abandoned channel?
	6	Horsetails, grasses, reeds, wetland
	7	Fine sand, < 10-year-old willows and alders, marginal logjam in river, 1 m above water level HWMs, fluvially deposited, unconsolidated
	8	Snags and downed wood, 60–200 cm DBH, bracken fern, deer fern, alders and conifers, young maples, ground topo dominated by root wads and their holes
	9	Overgrown channel with running water, horsetails, downed wood, small maple
	10	0.5 m deep and 4 m wide side channel, bracken fern, no water or mud
	11	20–60 cm DBH maples, abundant grass cover, bracken fern interspersed in grasses, undulating topo
	12	Up to 30 cm DBH alders, viny groundcover, between 2 side channels
	13	Muddy/silty overflow surface, on the channel side of a 1 m high cutbank (in the river), beaver chew
Sol Duc River	1	Fluvial surface, 2–3 m above water surface, covered with moss, ferns, widely spaced conifers, 30–250 cm DBH, bracken ferns, abundant downed wood, undulating topo under 1 *m*
	2	Sloping moss covered surface, closely spaced conifers, 6–15 cm DBH, small cobbles to boulders, some HWMs, terrace?
	3	Active channel
	4	Shallower slope than Class 2 from water level, small cobbles to boulders, <10 cm DBH alders, maples?, large leafy ground cover, maple up to 10 cm DBH, bracken ferns
	5	Overflow channel, evidence of recent competent flow, sparse moss on rocks, unconsolidated sediment, sand to large cobbles
	6	Off transect wetland/abandoned beaver pond: abundant vegetation, fern, large leafy ground cover, nurse logs, 20 cm DBH alders, sedges and rushes, side channel with flow in it, hellebore
	7	Ferns, devil's club, overgrown side channel, 0.5 m lower than previous patch, hellebore
	8	Small − 40 cm DBH abundant maples, abundant bracken ferns, nurse logs, small-30 cm DBH conifers, cobbles and boulders hiding under duff, undulating topo/linear features
	9	Abandoned side channel, overgrown ferns/grasses/maples, maple saplings, sand to cobble sized clasts
	10	3 + distinct channels, 20 cm DBH conifers, 40 cm DBH maples, 10–30 cm DBH alders, bracken fern, abundant groundcover including grasses, overflow surface including 2 + distinct channels, channels are ≤ to 1 m wide and have small cobbles to large boulders, log jam present
Lookout Creek	1	Active channel, ~2 m below Class 2, cobbles to boulders
	2	Debris flow/boulder bar, large gravel to boulder size clasts visible in bank cut, dense young veg, fir trees, viny maple, sword ferns, cedars, 2–20 cm DBH alders, beaver chew
	3	Backwater channel behind berm, multiple fern types, 3 m below top of Class 2, young viny maple, 8–30 cm DBH alder, standing water, sediment and coarse particulate organic matter build up, large nurse logs
	4	Backwater channel, 0.5 m above Class 3, abundant fern, abundant horsetail, deciduous plants, 10–30 cm DBH maple, undulating topo, gravel bars
	5	Abundant clover, downed wood, spaced out sword ferns, 10–100 cm DBH cedars/maple/fir
	6	Grassy side channel, 3 m wide, dry
	7	Cobble to boulder bar, mossy, dry, lower edges have dense viny maple, creek edge has dense willow
	8	Active side channel, 1.5 m wide, sand to boulders, leafy ground cover on banks, grassy banks, 1 m HWMs
	9	Overgrown side channel, thick layer of duff, 20–40 cm DBH fir and maple, clover
	10	Overflow cobble bank, dense willow, gentle slope from water surface, 50 cm HWMs
	11	Sandy riverbank between active channel and mossy terrace, 25 cm HWMs
	12	Overgrown surface, 5–15 cm DBH alder, groundcover, no flow (?)
	13	Active anastomosing island, beaver chew, very dense veg with willow, boulders underfoot, small side channels, viny maple
Altamaha River	0	Standing water with a little current, trees, some shrubs
	1	Small to 60 cm DBH conifers and deciduous trees, some undergrowth, but not dense; prolific leaf litter, bamboo, sparse palmettos, some vines. Sandy soil, pine needles, undulating topography with linear features
	2	Inundated, more palmetto, small to 60 cm DBH deciduous trees, no conifers in water, loam, silt, clay
	3	0.5 m vertical features, abundant palmettos, bamboo/small to 80 cm DBH trees, looks like wet recently (dark leaves and duff), linear features, viny, moss, no pine needles
	4	Similar to Class 3, but denser undergrowth, holly, palmettos, pine needles, same linear features as Class 3, bamboo
	5	Dry, pine needles, sandy, dense undergrowth, large palmettos, woody shrubs, a lot of conifers, 10–50 cm DBH, maples
	6	Small dense trees, interspersed old growth/large trees, dense leaf duff and pine needles, shrubs with big waxy leaves

Note: DBH stands for diameter at breast height, measured mostly by eye. Species identification was not exact and no field guide was used.

lidar-derived digital elevation models (DEMs) of equal to or better than 10 m spatial resolution retrieved from online portals (Division of Geology and Earth Resources., 2022; USGS, 2023b). DEM tiles were mosaicked in ArcGIS Pro where needed. A summary of all the data collected is provided in Table 3.

The field GPS locations of the transects, classes, and soil cores were brought into ArcGIS Pro (Esri, 2023) using the same tools as Iskin and Wohl (2023). The floodplains were delineated manually based on the transect locations and adjusted based on the Sentinel imagery and DEMs (Fig. 2). The Altamaha River study reach boundaries were chosen during data analysis as between a bounding road on the upstream end and just above a distributary section on the downstream end because of the aforementioned inundation during field work.

3.1. Classifications

Because our first objective is to make sense of the results from an unsupervised classification, we needed to modify the workflow from Iskin and Wohl (2023) to include more precise data that we could readily interpret. We also want to evaluate how the heterogeneity metrics calculated from the classified floodplains respond to the change in the underlying data, so we performed an ad hoc sensitivity analysis to qualitatively compare the two classifications. Going forward, Classification 1 will refer to the portion of this study that repeats the workflow from Iskin and Wohl (2023) for the Hoh River, Sol Duc River, Lookout Creek, and Altamaha River. Classification 2 will refer to the portion of this study that modifies the input data, is connected to the field data, and is interpretable (Objective 1).

Following the methods of Iskin and Wohl (2023), Classification 1 is performed with the four 10-m resolution bands from the Sentinel mosaics (red, green, blue, and near infrared) (Google Google Developers, 2022) and 10-m resolution DEMs from the U.S. Geological Survey's 3D Elevation Program (3DEP) (Table 3). Classification 2 is performed with the ten 10- and 20-m resolution bands from the Sentinel mosaics (red, green, blue, red edge 1–4, near infrared, and shortwave infrared 1–2) (Google Google Developers, 2022) and the highest resolution, publicly available DEMs we could obtain. We had access to 0.91-m (3-ft) resolution DEMs for the Hoh River and Lookout Creek and 3-m resolution DEMs for the Sol Duc River (Table 3). Prior to classification, all of the DEMs (for both Classification 1 and 2) were detrended and flattened following the same methods as Iskin and Wohl (2023) to accentuate the topography of the floodplains by removing the general downslope valley trends. We also calculated two index layers for the normalized difference vegetation index (NDVI) and normalized difference moisture index (NDMI) (Table 4). These indices can be used to differentiate vegetation and bare earth (USGS, 2018). The ArcGIS Pro tools *Make Raster Layer* and *Mosaic to New Raster* were used throughout to prepare the data for classification, and the *Indices* tool under the Imagery tab was used to create the NDVI and NDMI layers.

The *ISO Cluster Unsupervised Classification* tool was used to complete both Classification 1 and 2. The inputs for Classification 1 were the 4-band Sentinel mosaics and 10 m DEMs. The inputs for Classification 2 were the 10-band Sentinel mosaics, $\leq$ 10 m DEMs, NDVI layers, and NDMI layers. The tool also requires user input of (a) minimum class size in pixels, (b) sample size in pixels, and (c) maximum number of classes to find. Minimum class size was set to 4 pixels and sample size set to 2 pixels for both Classifications 1 and 2 at all sites. Maximum number of classes was set to 30 for the Altamaha and Hoh Rivers (large), 20 for the Sol Duc River (mid-sized), and 10 for Lookout Creek (small) for both Classifications 1 and 2. These values were chosen to increase the likelihood that the tool would find the maximum number of classes, and therefore more classes than we were able to observe in the field, without causing the tool to oversimplify. To demonstrate for Classification 1, when the maximum number of classes for Lookout Creek is set to 20, the tool finds 1 class, but when it is set to 10, it finds 10 classes. The tool seems to differentiate fewer classes if the maximum number of classes is set too high, with "too high" being found by trial and error.

Classified rasters, with "remote classes," were projected to the appropriate UTM zone using a cell size of 10 m with the *Project Raster* tool and exported for analysis using the *Copy Raster* tool. The suite of six heterogeneity metrics – aggregation index (aggregation), interspersion and juxtaposition index (interspersion), largest patch index (largest patch), patch density (density), percentage of like adjacencies (adjacencies), and Shannon's evenness index (evenness) – from Iskin and Wohl (2023) were calculated with the results from Classifications 1 and 2 in R (R Core Team, 2023). Symmetrized percent differences (SPD, denoted by s%) (Eq. (1) were calculated for each metric as an ad hoc sensitivity analysis comparing the results between Classifications 1 and 2 (Nuzzo, 2018) (absolute value added to maintain positive values). Lastly, the spatial heterogeneity values from Washington, Oregon, and Georgia were compared qualitatively to those from Colorado and Oklahoma in Iskin and Wohl (2023) (Objective 3).

$$Symmetrized\ Percent\ Difference\ (s\%) = \left(\frac{|Class\ 1\ Metric - Class\ 2\ Metric|}{Class\ 1\ Metric + Class\ 2\ Metric}\right) \times 100 \quad (1)$$

3.2. Interpretation

Natural floodplains vary greatly in the U.S. by region, elevation, and watershed position. We chose an unsupervised classification because this natural variation makes it unreasonable to train a supervised classifier. The field classes observed in coastal Georgia, for example, may be very different from those observed in inland Oregon even though both are active natural floodplains. An unsupervised classification workflow allows for comparison of general, landscape-level heterogeneity across the U.S. without having to know exactly what the classes are. This raised the question of what the remote classes actually represent. This is where the field observations are useful. Alhough not required to complete the classifications just described, the field classes are necessary for interpreting the remote classes.

Objective 2 focusses on using the underlying data from Classification 2 and the field data to increase the interpretability of the remote classes. To do this, we mined the underlying remote sensing data, summarized values for each remote class, and spatially related the remote classes to the field classes.

To mine and summarize the remote data, detrended-flattened elevations, NDVI, and NDMI, and remote class numbers were extracted to random points using the *Extract Multi Values to Points* tool (random points that have an approximate point density of 100 pts/ha). The elevation data were "un-flattened" by dividing the values by 0.1 so that they were more representative of real elevations and therefore more interpretable. To spatially connect the field and remote classes, field class lines and soil core points were joined within a specified geodesic distance to the extracted remote class random point data using the "One to Many" option of the *Spatial Join* tool. Field classes were joined within 3 m of remote classes and soil cores were joined within 10 m of remote classes. A greater distance was used for the core data because there were fewer core data than field class data. This process creates a few extracted/joined tables for each site, and those were exported to Excel for analysis. Pivot tables were used to calculate the average detrended elevation, NDVI, and NDMI for each remote class for each river. The nearest field class and soil core data were compared manually to the remote classes as one remote class point might be within 3 m of more than one field class line and/or within 10 m of more than one soil core point. Remote classes were then interpreted for each of the four field sites based on elevation, NDVI, nearest field classes, nearest soil textures and moistures, and visual inspection of imagery in ArcGIS Pro and Google Earth.

Table 3
Data collected and used in this analysis for the Hoh River, Washington (HWA); the Sol Duc River, Washington (SDWA); Lookout Creek, Oregon (LOR); and the Altamaha River, Georgia (AGA).

	Data	Details	Instrument	Resolution	Program Used	References
Field Data	GPS Locations	Patch boundaries and sediment cores	Garmin GPSMAP 66ST	± 3 *m*	–	–
	Soil Data	Soil texture data provided in % sand, % silt, and % clay (HWA, SDWA, LOR) Not available for AGA	JMC Soil Samplers 15 in Wet Sampling Tube (2.2 cm diameter)	± 3 m horizontal (GPS) ~30 cm maximum vertical (corer size)	–	–
	Cloud-free Mosaics*	2 % cloudy mean pixels from 5/1/2022–9/30/2022 (HWA, SDWA, LOR) 0.5 % cloudy mean pixels from 4/1/2022–9/30/2022 (AGA)	Copernicus Sentinel-2A	10 m: Bands 2, 3, 4, 8 20 m: Bands 5, 6, 7, 8a, 11, 12 12-bit radiometric 5-day temporal	Google Earth Engine	ESA, 2021; Google Developers, 2022; Gorelick et al., 2017; Sabins Jr. & Ellis, 2020
	Digital Elevation Models	Tile N48W124 5/5/2022 (HWA, SDWA) Tile N48W125 1/9/2020 (HWA, SDWA) Tile N49W124 1/9/2020 (HWA, SDWA) Tile N45W123 4/26/2022 (LOR) Tile N32W082 7/25/2022 (AGA)	Airborne Lidar	1/3 arc-second 1 x 1 degree 10 *m*	The National Map	Open Topography, 2021; USGS, 2023b
	High-Resolution Digital Elevation Models	Hoh River 2013 DEM 4, 5 Sol Duc River 2014 DEM 47, 57 McKenzie River 2016 DEM mosaic Not available for AGA	Airborne Lidar	3 ft (HWA and LOR) 3 m (SDWA) 32-bit radiometric	WA DNR Lidar Portal	U.S. Geological Survey (USGS), 2016; Allison and Martinez, 2013; Division of Geology and Earth Resources., 2022; Gleason and McWethy, 2014

* Note: The cloudy percentage was decreased by 1.5 % and the date range was lengthened by one month for the Altamaha River because of high cloud cover in the region.

4. Results

We first present the results from Classification 1 and 2 that show the mapped patches and classes from the unsupervised classification workflow. We then present the calculated heterogeneity metrics and compare them between Classification 1 and 2, and between geographic locations. Lastly, we present the results of the class interpretation for the four river floodplains.

4.1. Classifications

Resulting rasters from Classifications 1 and 2 for all field sites are shown in Fig. 4 and Fig. 5, respectively. Visual inspection shows that the results from Classification 2 may be less patchy than those from Classification 1 (Fig. 4a and 5a), and that increasing the spatial resolution of the DEM probably led to better classification of the shape of the channel for the Sol Duc River (Fig. 4b and 5b).

The heterogeneity metrics calculated for the four rivers for both classifications are given in Table 5 and visualized in Fig. 6. We used the same qualitative high-moderate-low scale as Iskin and Wohl (2023), in which high is assigned to metric values in the top 75 % of their range, moderate to values in the middle 50 % of their range, and low to values in the bottom 25 % of their range. All four sites exhibit moderate aggregation (Fig. 6a,g) and moderate adjacencies (Fig. 6e,k) for both Classifications 1 and 2. The Altamaha, Hoh, and Sol Duc Rivers exhibit low values of largest patch (Fig. 6c,i) and high evenness (Fig. 6f,l) for both classifications. The Hoh and Altamaha Rivers exhibit moderate interspersion (Fig. 6b,h), whereas the Sol Duc River exhibits high interspersion (Fig. 6b,h) for both classifications. Lookout Creek exhibits high interspersion (Fig. 6b), low largest patch (Fig. 6c), and high evenness for Classification 1 (Fig. 6f), but moderate interspersion (Fig. 6h), moderate largest patch (Fig. 6i), and moderate evenness for Classification 2 (Fig. 6l). Lookout Creek is the only river for which metrics change qualitatively between Classification 1 and 2, with a decrease from high interspersion and evenness to moderate and an increase from low to moderate largest patch.

Table 6 shows the results of the ad hoc sensitivity analysis. Largest patch and density have the highest median SPD of the metrics, whereas evenness has the smallest median SPD. Lookout Creek has the highest SPD for all metrics, whereas the other three rivers have generally similar and lower SPD.

These results indicate that these natural rivers have moderately aggregated classes and moderate aggregation within the classes; moderate to high intermixing; low to moderate dominance of the largest patch; and moderately to highly abundant, evenly distributed classes (Hesselbarth et al., 2021). Rivers of the Pacific Northwest and Southeast have similar aggregation and evenness as rivers in Colorado and Oklahoma, but lower intermixing (Iskin & Wohl, 2023). Rivers on the Olympic Peninsula (Hoh and Sol Duc Rivers) and in the Southeast (Altamaha River) have similar spatial heterogeneity as beaver-modified and shortgrass prairie rivers in Colorado, whereas the more inland Lookout Creek of Oregon has similar spatial heterogeneity to Sand Creek in the tallgrass prairie of Oklahoma (Iskin & Wohl, 2023).

4.2. Interpretation

Remote classes were grouped starting with high positive class-average elevations. We used general thresholds and ranges of NDVI values from the U.S. Geological Survey (2018) and visual inspection to further group remote classes. Nearest soil textures and moisture and nearest field classes were used to validate the groupings and provide geomorphic units, vegetation ages, and species types (Table 2). Fig. 7 visualizes the interpreted remote classes from Supplemental Tables 1-4.

For the Hoh River, blue represents the bare sediment, water, and/or sparsely vegetated midchannel islands in and around the active channel; light green represents the active floodplain with channel features, wetlands, younger forest and groundcover, and varying vegetation health/density; dark green represents old-growth forest floor/inactive

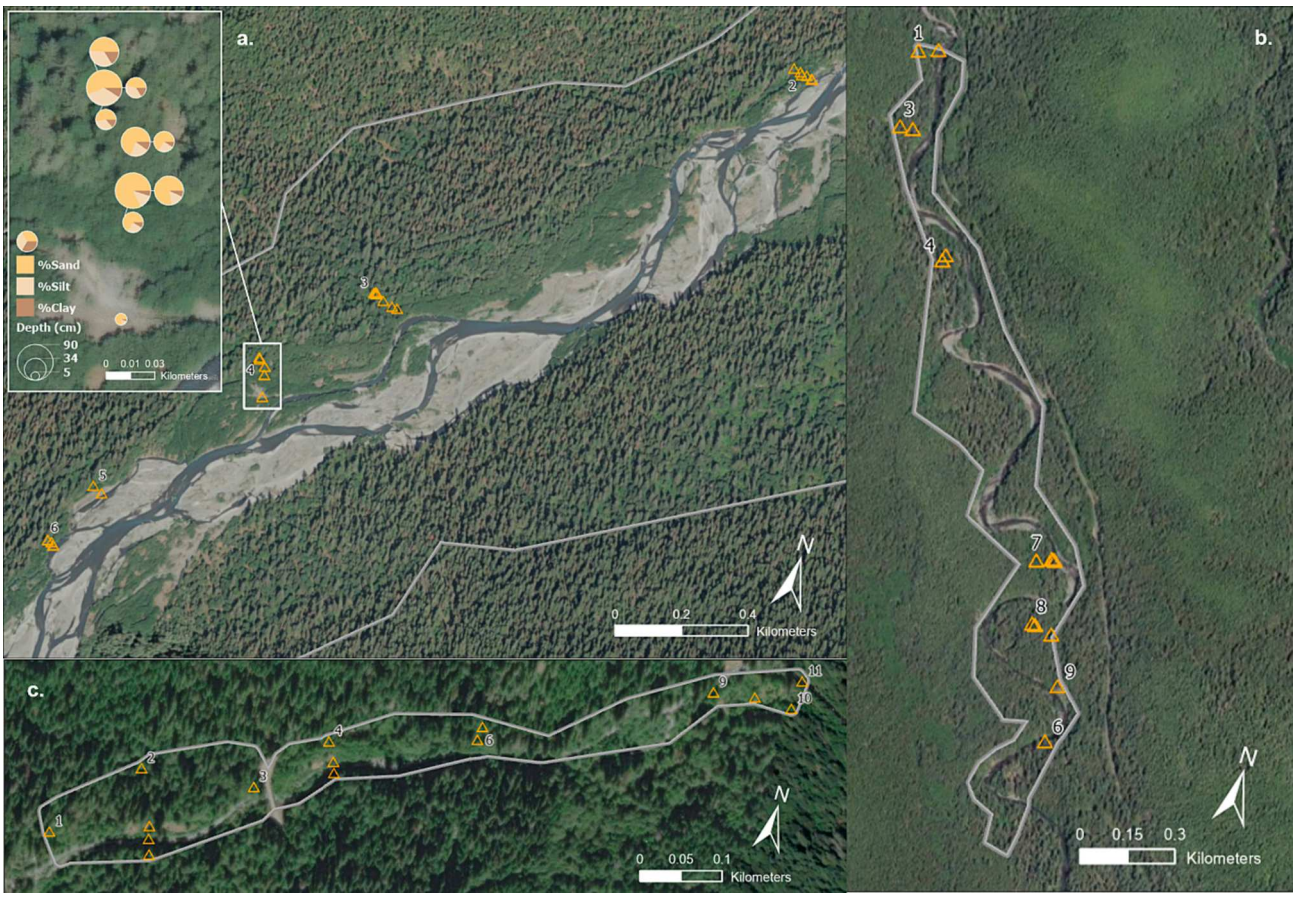

Fig. 3. Locations of soil cores (orange triangles) within mapped floodplain boundaries (grey lines) for a) the Hoh River, Washington with inset; b) the Sol Duc River, Washington; and c) Lookout Creek, Oregon. Inset for the Hoh River demonstrates the fractional soil components for transect 4 on river river-right. Pie chart colors indicate soil components and size indicates core depth below the surface. The base map is the Imagery layer from ArcGIS Pro (Esri, 2023). (For interpretation of the references to colour in this figure legend, the reader is referred to the web version of this article.)

Table 4
Data layers created from the cloud-free mosaics using ArcGIS Pro.

Value	Band Ratio	Spatial Resolution	Interpretation	References
NDVI	$\frac{B8-B4}{B8+B4}$	10 *m*	Range [-1, 1], indicator of vegetation greenness, health, and/or density; higher values indicate healthier/greener/denser vegetation	EOS Data Analytics, 2019; GISGeography., 2022a; GISGeography., 2022b; Google Developers, 2022; USGS, 2018, 2022a, 2022b
NDMI	$\frac{B8a-B11}{B8a+B11}$	20 *m*	Range [-1, 1], indicator of vegetation moisture content; higher values indicate vegetation with more water	

floodplain with nurse logs and varying vegetation health/density of mosses, fern (including *Polystichum* and *Athyrium* spp.), alder (*Alnus* spp.), conifer (including *Picea*, *Pseudotsuga*, and *Thuja* spp.), and maple (*Acer* spp.) (NPS, 2015, 2020); and beige represents uplands and inactive floodplain with varying vegetation health/density (Fig. 7a). For the Sol Duc River, blue represents the active channel; light green represents the active floodplain, and/or vegetation overhanging channel, with side channels, overflow surfaces, nurse logs, and varying vegetation health/density, including mosses, alder, maple, herbaceous groundcover, fern, conifer, and grasses; and beige represents higher elevation surfaces and/or uplands with conifer forest, including vertical cliffs above the channel (Fig. 7b). For Lookout Creek, light green represents the active channel and floodplain with midchannel island, boulder bars, backwater channels, side channels and varying vegetation health/density, including fir, viny maple, fern, cedar, alders, horsetail (*Equisetum* spp.), grasses, and evidence of beaver chew (OSU, 2023); and grey represents the bridge, road, steep banks and/or boundaries next to channel and floodplain (Fig. 7c). Lastly, for the Altamaha River, blue represents the active channel, tributaries, side channels, and/or standing water; light green represents the Active floodplain with inundated areas and areas of exposed sediment, varying vegetation health/density, including evergreen and deciduous trees (including *Pinus*, *Quercus*, *Taxodium*, and *Ulmus* spp.), bamboo, palmetto (*Serenoa* spp.), moss, vines, leaf litter, holly (*Ilex* spp.), and maples (*Acer* spp.) (Luber, 2002); and grey represents structures, roads, other manmade surfaces, and/or active floodplain with similar spectral properties (Fig. 7d).

5. Discussion

Extraction of the underlying data was necessary for interpreting the remote classes. We find that class-averaged NDVI is an effective differentiator of vegetation vs. non-vegetation floodplain surfaces. Although NDMI seems to follow the same trend as NDVI, NDMI data are harder to interpret but seem to improve the classifications. The field data are

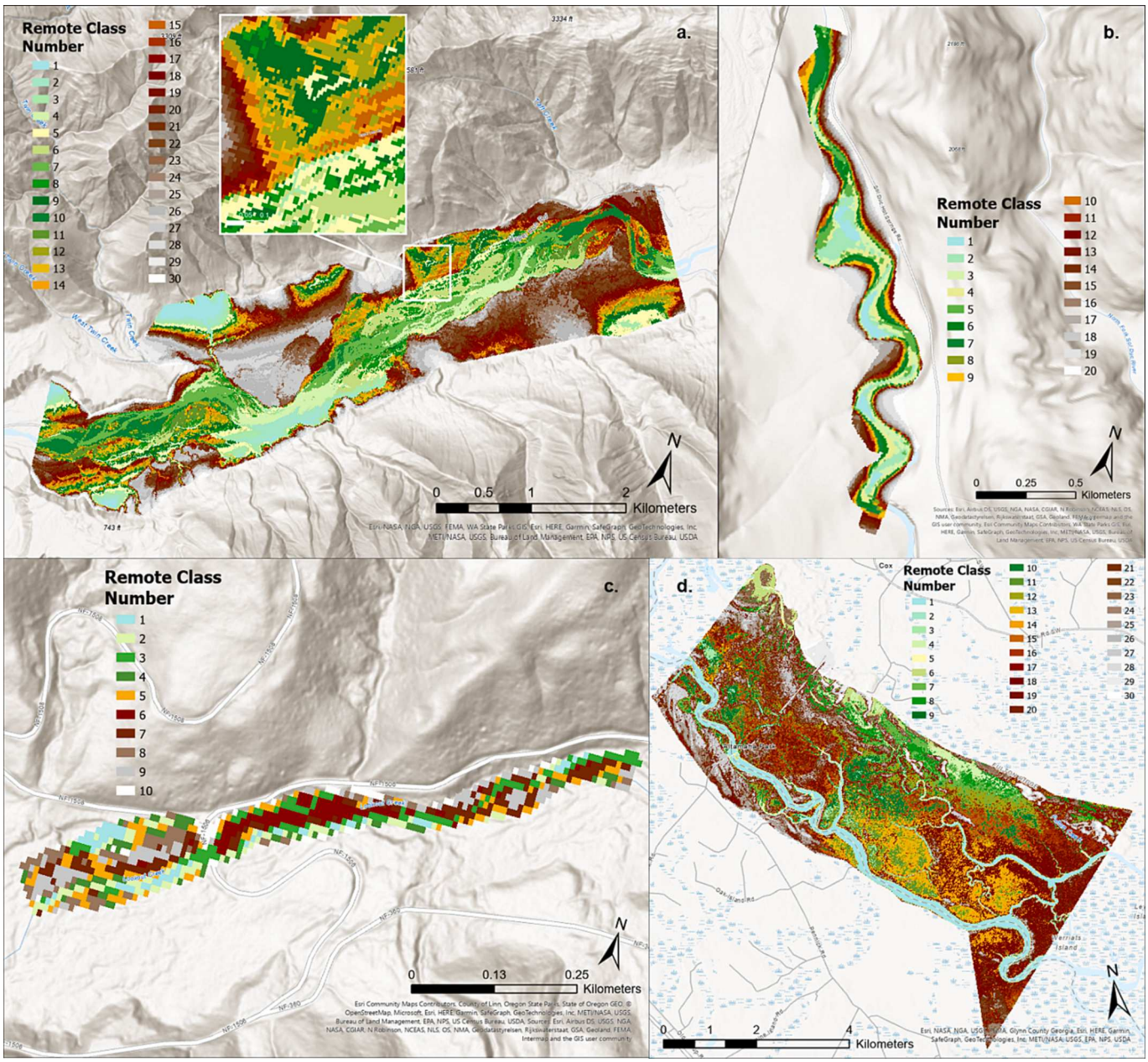

Fig. 4. Unsupervised classifications results from Classification 1 for the a) Hoh River, Washington with detail inset, b) Sol Duc River, Washington, c) Lookout Creek, Oregon, and d) Altamaha River, Georgia. Classification completed with 4-band Sentinel-2A imagery and detrended, flattened DEMs. Remote class numbers are separate from field class numbers.

crucial for differentiating between different types of floodplain classes. We were able to differentiate between younger active floodplain and older floodplain for the Hoh River (Fig. 7a) because of the field descriptions, but we could not further differentiate for the Altamaha River (Fig. 7d) because of the unexpected inundation and lack of ground access to the floodplain. Although we were able to group remote classes into geomorphic units, the groups gloss over the inherent heterogeneity of the individual classes. The groups are visually interesting and generally interpretable, but we propose that it is the heterogeneity within the groups that is vital to floodplain functioning. For example, the grouped light green younger active floodplain at the Hoh River (Fig. 7a) includes side channels, but the individual channels in which fluvial processes such as water, sediment, organic matter transport and provision of habitat occur are not actually visible. The classifications give us more insight to the structure and function of the floodplains than do the groupings.

Although interspersion differs qualitatively between sites, aggregation, largest patch, and evenness do not differ between sites or classifications for the Altamaha, Hoh, and Sol Duc Rivers. This indicates that perhaps the metrics are more influenced by actual properties of the floodplains and less by the data used. This is encouraging, especially as there was a mismatch in resolution between the Hoh River and Lookout DEMs (0.9 m), the Sol Duc River DEM (3 m), and the Altamaha River DEM (10 m) for Classification 2. This indicates the value of using the highest available resolution for elevation data. This is exemplified in the results for the Sol Duc River (Fig. 4b vs. Fig. 5b). We find that the increased spatial resolution is most important for the smallest rivers, as each pixel covers a greater percentage of the floodplain for smaller rivers and therefore less granularity is possible per pixel than for larger rivers. For broad comparison studies, we suggest using aerial imagery with the same spectral imagery for all sites and the highest available resolution of topographic data. The heterogeneity metrics differ qualitatively for

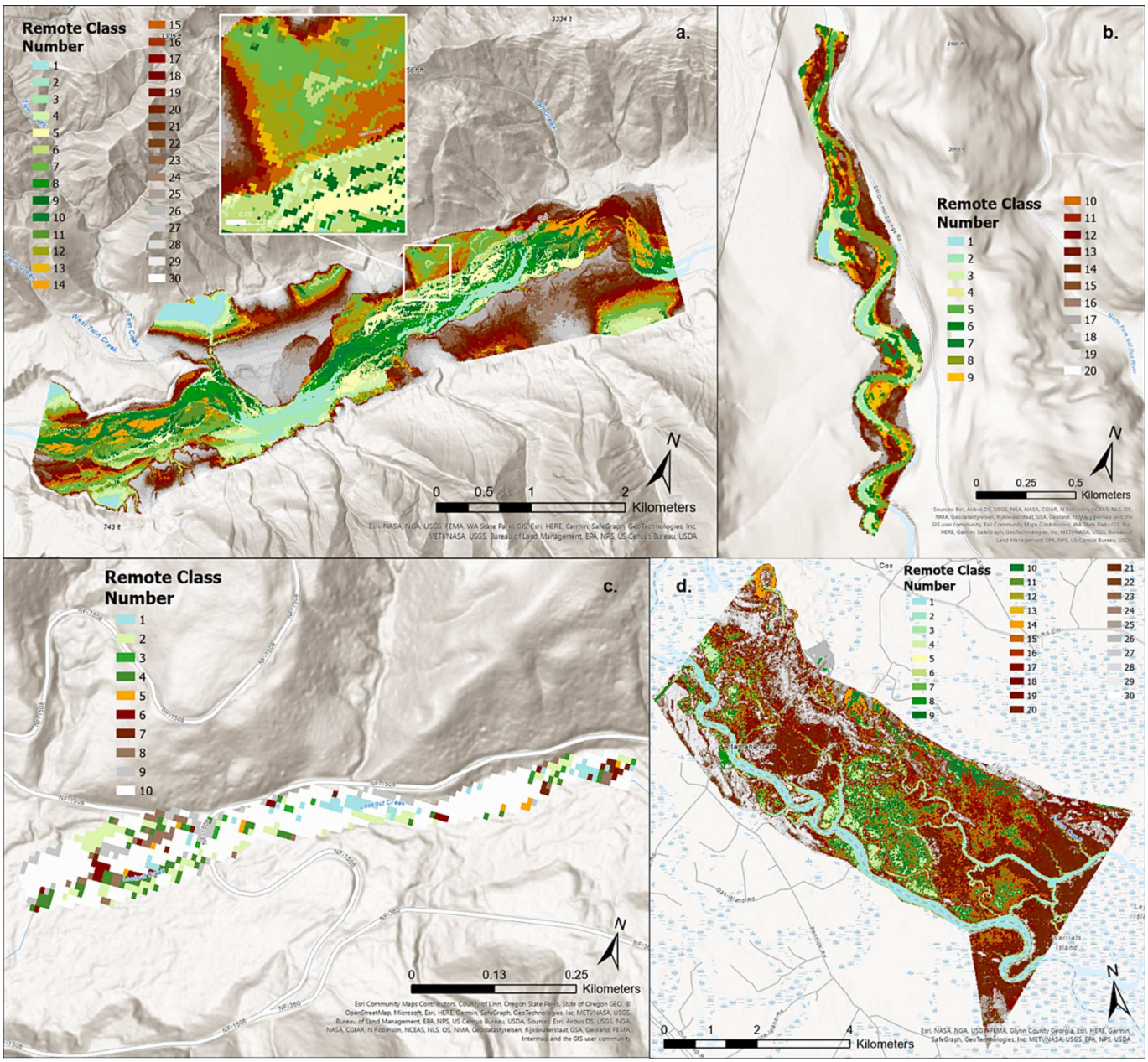

Fig. 5. Unsupervised classifications results from Classification 2 for the a) Hoh River, Washington with detail inset, b) Sol Duc River, Washington, c) Lookout Creek, Oregon, and d) Altamaha River, Georgia. Classification completed with 10-band Sentinel-2A imagery, detrended, flattened high resolution DEMs where available, NDVI, and NDMI. Remote class numbers are separate from field class numbers.

Table 5
Values of landscape heterogeneity metrics for Classification 1 and 2.

Metric	Aggregation (%)		Interspersion (%)		Largest patch (%)		Density (#/100 ha)		Adjacencies (%)		Evenness	
Classification	*1*	*2*	*1*	*2*	*1*	*2*	*1*	*2*	*1*	*2*	*1*	*2*
Altamaha River	56.2	58.8	73.8	73.3	6.4	4.2	1355.2	1213.0	55.9	58.5	0.946	0.934
Hoh River	62.3	66.0	73.8	71.6	1.7	1.6	1043.7	855.3	61.6	65.3	0.980	0.973
Sol Duc River	53.5	50.8	76.3	79.9	3.3	2.0	1576.7	1866.4	52.2	49.5	0.979	0.967
Lookout Creek	39.5	57.4	88.8	74.9	8.7	26.1	2662.7	1697.5	38.5	58.6	0.982	0.639

Lookout Creek between Classification 1 and 2. This could be because the floodplain is small and adjustment to pixel values alters the results dramatically. With this in mind, we propose that using the same spectral data when comparing classifications between sites is an important step in the workflow. Moving forward with similar analyses of additional sites, we suggest the removal of largest patch from the suite of heterogeneity metrics because it appears to be dependent on the classification input data and has variable and sometimes large SPD across the rivers (49.9 % for Lookout Creek). We suggest using the smaller suite of five metrics: aggregation, interspersion, density, adjacencies, and evenness.

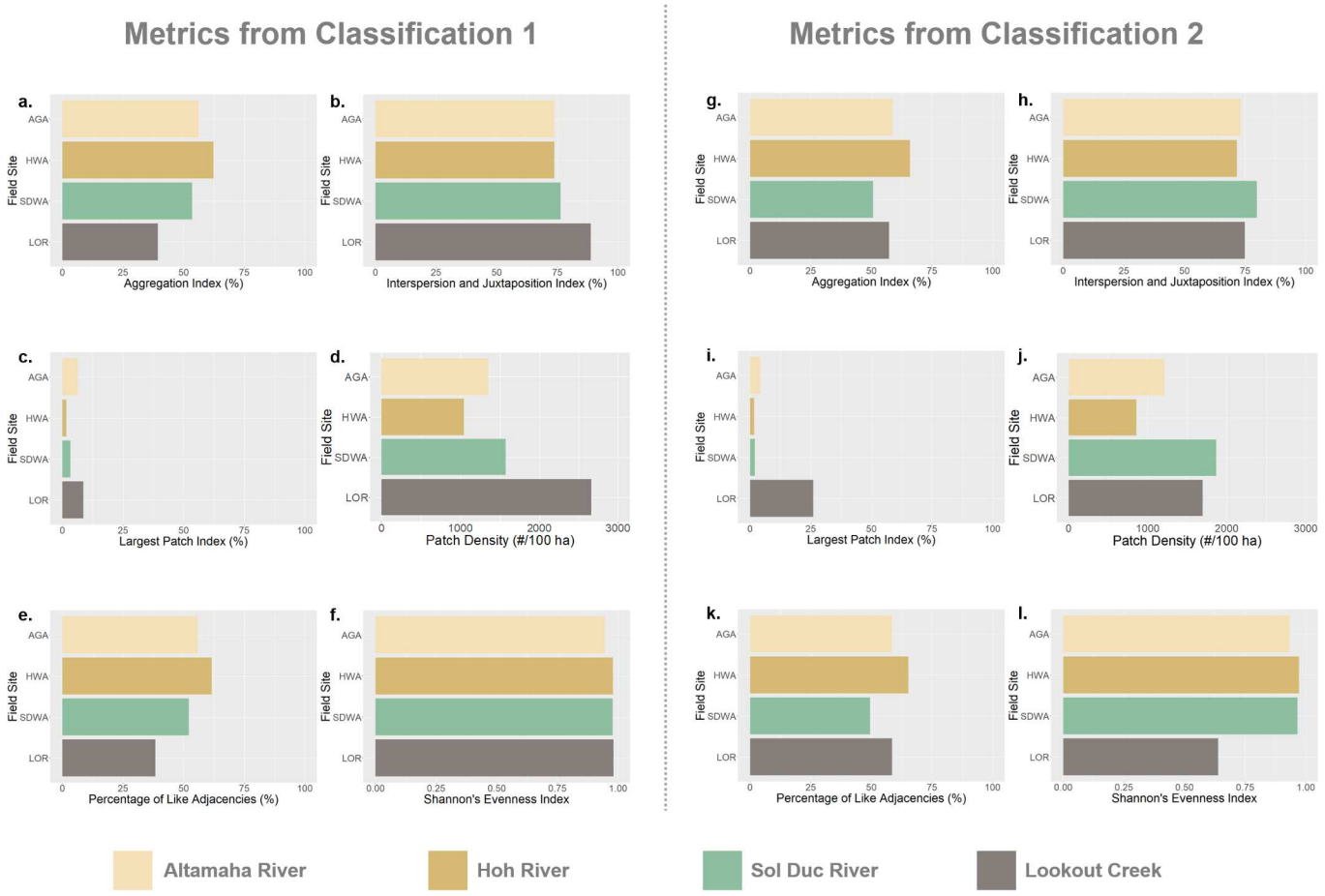

Fig. 6. Bar plot visualizations of the levels of each metric for each floodplain for Classification 1 (a-f) and Classification 2 (g-l). In descending order of upstream drainage area, cream bars represent the Altamaha River, Georgia, gold bars represent the Hoh River, Washington, green bars represent the Sol Duc River, Washington, and grey bars represent Lookout Creek, Oregon. (For interpretation of the references to colour in this figure legend, the reader is referred to the web version of this article.)

Table 6
Symmetrized percent difference (SPD) between Classification 1 and 2.

Metric	Altamaha River	Hoh River	Sol Duc River	Lookout Creek	Median SPD
Aggregation	2.3 s%	2.9 s%	2.6 s%	18.5 s%	2.7 s%
Interspersion	0.4 s%	1.5 s%	2.3 s%	8.5 s%	1.9 s%
Largest patch	21.0 s%	1.8 s%	24.5 s%	49.9 s%	22.8 s%
Density	5.5 s%	9.9 s%	8.4 s%	22.1 s%	9.2 s%
Adjacencies	2.3 s%	2.9 s%	2.7 s%	20.7 s%	2.8 s%
Evenness	0.6 s%	0.4 s%	0.6 s%	21.1 s%	0.6 s%

Note: Colors indicate level of change, where red is a change of 50 %, yellow is a change of 25 %, and green is a change of 0 %.

Overall, the results suggest that natural floodplains in the Pacific Northwest and coastal Southeast regions of the United States have similar aggregation and evenness as rivers in Colorado and Oklahoma, but lower intermixing (Iskin & Wohl, 2023). The results show that the larger rivers in this study (Altamaha, Hoh, and Sol Duc Rivers) have similar spatial heterogeneity as beaver-modified and shortgrass prairie rivers in Colorado, whereas the more inland and smaller river (Lookout Creek) has similar spatial heterogeneity to the tallgrass prairie site (Sand Creek) (Iskin & Wohl, 2023).

We calculated the ratio of average floodplain width to average channel width in ArcGIS Pro from six hand-drawn, approximately evenly spaced cross sections at each river using the Sentinel imagery, floodplain boundaries, and field delineations. The ratio of floodplain width to channel width is 19.3 for the Altamaha River, 7.0 for the Hoh and Sol Duc Rivers, and 3.2 for Lookout Creek. We attribute the lower interspersion at the Altamaha River compared to the Sol Duc River, and West Bijou, East Plum, and Rough and Tumbling Creeks to slower rates of lateral channel migration or avulsion across the much broader floodplains (Konrad, 2012). The Hoh River has lower interspersion than the Sol Duc River despite the same average floodplain to channel width ratio. We attribute this to the different hydrologic and sediment regimes on either side of the Olympic Mountains. The Hoh River valley is a temperate rainforest (NPS, 2020) that is glacially fed and receives almost twice as much precipitation as the Sol Duc River valley (Table 1). The Sol Duc River valley is a lowland forest (NPS, 2015) and is lake-fed. These differences in precipitation and source flow could result in different sediment regimes (Wada et al., 2011), as well as the braided planform seen at the Hoh River and not at the Sol Duc River. The more dynamic planform of the braided Hoh River (Sambrook Smith et al., 2006) could result in the higher pairing of certain classes (lower

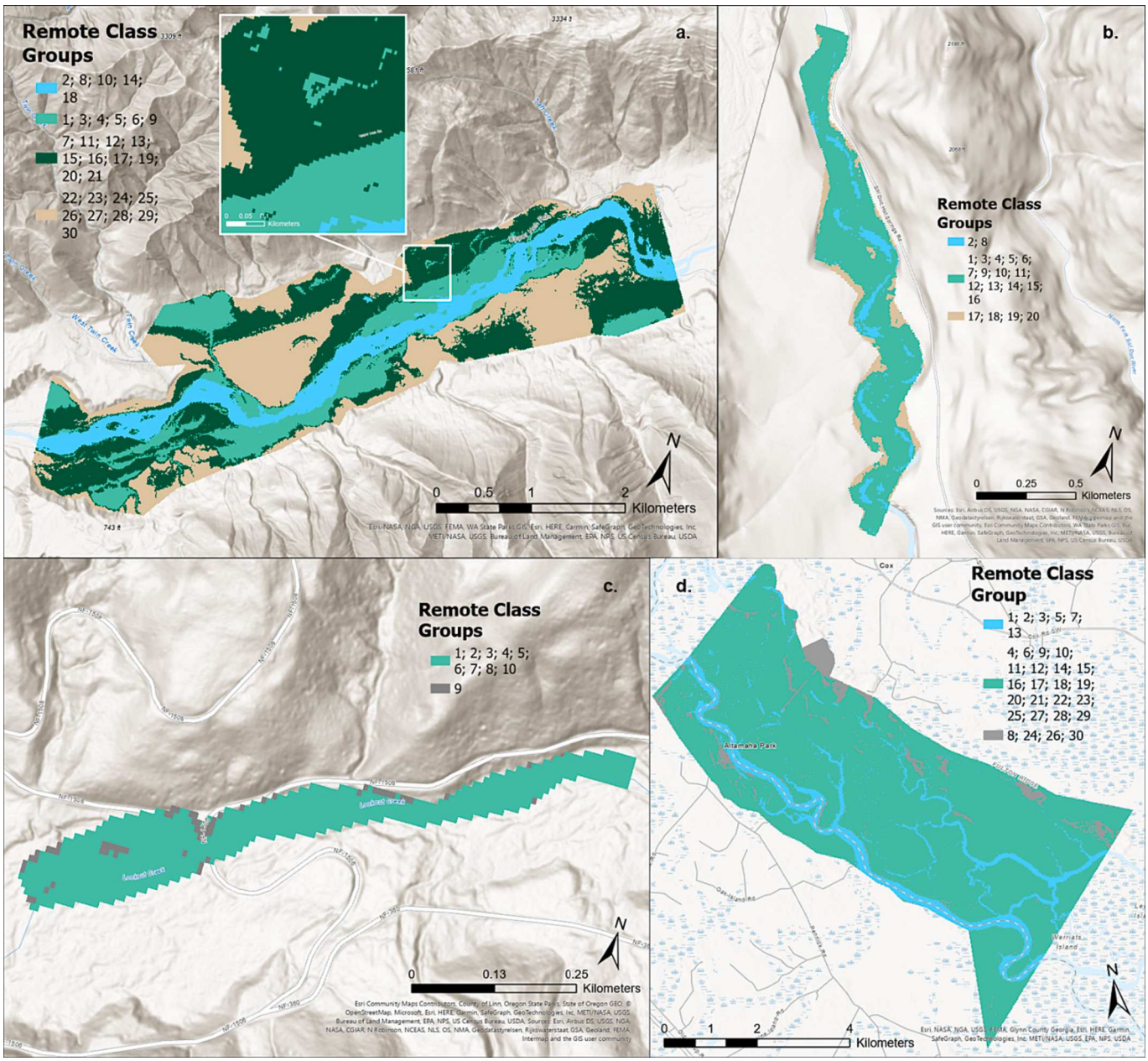

Fig. 7. Grouped remote classes based on class-averaged detrended elevation, NDVI, NDMI and nearby field classes and soil cores for the a) Hoh River, Washington with detail inset, b) Sol Duc River, Washington, c) Lookout Creek, Oregon, and d) Altamaha River, Georgia.

interspersion) by more punctuated/less gradual channel movement across the floodplain (Schumm, 1985). We attribute the high evenness at the Altamaha, Hoh, and Sol Duc Rivers to the natural flow, sediment, and wood regimes, as did Iskin and Wohl (2023) in the earlier analysis of West Bijou, East Plum, and Rough and Tumbling Creeks. We attribute the similarities of aggregation and intermixing between Lookout Creek (Classification 1) and Sand Creek to lateral confinement of the channels and low ratio of average floodplain width to average channel width at Lookout Creek.

6. Conclusion

We repeated a previously developed unsupervised classification workflow for rivers in the U.S. Pacific Northwest and Southeast, and compared the results based on data used and metrics calculated. Field observations and increased precision of remote data allowed us to make general groupings of remote classes. Our results indicate that natural floodplains in the Pacific Northwest and coastal Southeast have moderate to high evenness, moderate to high intermixing, and moderate aggregation; and similar aggregation and evenness as rivers in Colorado and Oklahoma, but lower intermixing. We attribute lower intermixing at the Altamaha River to slower rates of lateral channel migration, and lower intermixing at the Hoh River to the different hydrologic and sediment regimes and less stable braided planform. The results show that the larger rivers in this study (Altamaha, Hoh, and Sol Duc Rivers) have similar spatial heterogeneity as beaver-modified and shortgrass prairie rivers in Colorado, whereas the more inland and smaller river (Lookout Creek) has similar spatial heterogeneity to the tallgrass prairie site (Sand Creek).

Our results also indicate that using the highest resolution topographic data available and the same spectral resolution aerial imagery is the best path forward when comparing results between sites. The metrics show that there are similarities and differences between rivers in Washington, Oregon, Colorado, Oklahoma, and Georgia, and that

discernable trends may arise from a meta study comparing heterogeneity from more rivers across the country.

Declaration of competing interest

The authors declare the following financial interests/personal relationships which may be considered as potential competing interests: Ellen Wohl and Emily Iskin report financial support was provided by Colorado Parks and Wildlife. Emily Iskin reports financial support was provided by Geological Society of America, American Water Resources Association Colorado, and Colorado Scientific Society.

Data availability

Data has been published and can be accessed at: https://doi.org/10.5061/dryad.0k6djhb4q

Acknowledgements

The authors thank Colorado Parks and Wildlife, the Geological Society of America, American Water Resources Association Colorado, and the Colorado Scientific Society for funding awarded to this project. We would also like to thank Samantha Pearson and Olivia Cecil for field work assistance, and we acknowledge the National Park Service for access to Olympic National Park under permit OLYM-2021-SCI-0044 and Max Ross for providing provisional soil data for the Hoh and Sol Duc Rivers. Facilities were provided by the HJ Andrews Experimental Forest and Long Term Ecological Research (LTER) program, administered cooperatively by Oregon State University, the USDA Forest Service Pacific Northwest Research Station, and the Willamette National Forest. We also acknowledge Christi Lambert with The Nature Conservancy for assistance with background information for and access at the Altamaha River. The manuscript benefited from comments by two anonymous reviewers.

Appendix A. Supplementary data

Supplementary data to this article can be found online at https://doi.org/10.1016/j.jhydrol.2023.130508.

References

Aguiar, F.C., Ferreira, M.T., Albuquerque, A., Rodríguez-González, P., Segurado, P., 2009. Structural and functional responses of riparian vegetation to human disturbance: Performance and spatial scale-dependence. Fundam. Appl. Limnol. 175 (3), 249–267. https://doi.org/10.1127/1863-9135/2009/0175-0249.

Allison, S., & Martinez, D. (2013). *Hoh River LiDAR-Delivery 2 Technical Data Report.*

Appling, A.P., Bernhardt, E.S., Stanford, J.A., 2014. Floodplain biogeochemical mosaics: A multidimensional view of alluvial soils. J. Geophys. Res. Biogeo. 119 (8), 1538–1553. https://doi.org/10.1002/2013JG002543.

Collins, B.D., Montgomery, D.R., Fetherston, K.L., Abbe, T.B., 2012. The floodplain large-wood cycle hypothesis: A mechanism for the physical and biotic structuring of temperate forested alluvial valleys in the North Pacific coastal ecoregion. Geomorphology 139–140, 460–470. https://doi.org/10.1016/j.geomorph.2011.11.011.

Rand Mcnally And Company, & Seaboard Air Line Railroad Company (Mcnally & Seaboard). (1896) *Map of the Seaboard Air Line and its principal connections north, south, east & west.* Chicago, 1896. [Map] Retrieved from the Library of Congress, https://www.loc.gov/item/98688799/.

EOS Data Analytics, Inc. (2019, August 30). NDVI FAQ: All You Need To Know About Index. https://eos.com/blog/ndvi-faq-all-you-need-to-know-about-ndvi/.

Google Developers, 2022. Sentinel-2 MSI: MultiSpectral Instrument, Level-2A. Earth Engine Data Catalog. https://developers.google.com/earth-engine/datasets/catalog/COPERNICUS_S2_SR.

Fetherston, K.L., Naiman, R.J., Bilby, R.E., 1995. Large wood debris, physical process, and riparian forest development in montane networks of the Pacific Northwest. Geomorphology 13 (1–4), 133–144. https://doi.org/10.1016/0169-555X(95)00033-2.

Division of Geology and Earth Resources. (2022). *Washington Lidar Portal.* Washington State Department of Natural Resources. https://lidarportal.dnr.wa.gov/.

Esri. (2023). *ArcGIS Pro*. https://www.esri.com/en-us/arcgis/products/arcgis-pro/overview.

European Space Agency (ESA). (2021). *Level-2A*. Sentinel Online. https://sentinel.esa.int/web/sentinel/user-guides/sentinel-2-msi/product-types/level-2a.

GISGeography. (2022a, May 30). *What is NDVI (Normalized Difference Vegetation Index)?* https://gisgeography.com/ndvi-normalized-difference-vegetation-index/.

GISGeography. (2022b, June 4). *Sentinel 2 Bands and Combinations*. https://gisgeography.com/sentinel-2-bands-combinations/.

Gleason, A., & McWethy, G. (2014). Lidar Project Quality Assurance Report. https://www.dnr.wa.gov/geology.

Gorelick, N., Hancher, M., Dixon, M., Ilyushchenko, S., Thau, D., Moore, R., 2017. Google Earth Engine: Planetary-scale geospatial analysis for everyone. Remote Sens. Environ. 202, 18–27. https://doi.org/10.1016/j.rse.2017.06.031.

Gostner, W., Alp, M., Schleiss, A.J., Robinson, C.T., 2013. The hydro-morphological index of diversity: A tool for describing habitat heterogeneity in river engineering projects. Hydrobiologia 712, 43–60. https://doi.org/10.1007/s10750-012-1288-5.

Helton, A.M., Poole, G.C., Payn, R.A., Izurieta, C., Stanford, J.A., 2014. Relative influences of the river channel, floodplain surface, and alluvial aquifer on simulated hydrologic residence time in a montane river floodplain. Geomorphology 205, 17–26. https://doi.org/10.1016/j.geomorph.2012.01.004.

Hesselbarth, M. H. K., Sciaini, M., Nowosad, J., Hanss, S., Graham, L. J., Hollister, J., & With, K. A. (2021). Package "landscapemetrics" Reference Manual. https://cran.r-project.org/web/packages/landscapemetrics/.

Horton, J.D., 2017. The State Geologic Map Compilation (SGMC) Geodatabase of the Conterminous United States (1.1). U.S. Geologic Survey. https://doi.org/10.5066/F7WH2N65.

Horton, J. D., San Juan, C. A., & Stoeser, D. B. (2017). *The State Geologic Map Compilation (SGMC) geodatabase of the conterminous United States (ver. 1.1, August 2017).* https://doi.org/10.3133/ds1052.

Hugue, F., Lapointe, M., Eaton, B.C., Lepoutre, A., 2016. Satellite-based remote sensing of running water habitats at large riverscape scales: Tools to analyze habitat heterogeneity for river ecosystem management. Geomorphology 253, 353–369. https://doi.org/10.1016/j.geomorph.2015.10.025.

Iskin, E.P., Wohl, E., 2023. Quantifying floodplain heterogeneity with field observation, remote sensing, and landscape ecology: Methods and metrics. River Res. Appl. 39 (5), 911–929. https://doi.org/10.1002/rra.4109.

Knox, R.L., Morrison, R.R., Wohl, E.E., 2022a. A river ran through hit: Floodplains as America's newest relict landform. *Science*. Advances 8 (25), eabo1082. https://doi.org/10.1126/sciadv.abo1082.

Knox, R.L., Wohl, E.E., Morrison, R.R., 2022b. Levees don't protect, they disconnect: A critical review of how artificial levees impact floodplain functions. Sci. Total Environ. 837, 155773 https://doi.org/10.1016/j.scitotenv.2022.155773.

Konrad, C.P., 2012. Reoccupation of floodplains by rivers and its relation to the age structure of floodplain vegetation. *Journal of Geophysical Research*. Biogeosciences 117 (G4). https://doi.org/10.1029/2011JG001906.

Kuiper, J.J., Janse, J.H., Teurlincx, S., Verhoeven, J.T.A., Alkemade, R., 2014. The impact of river regulation on the biodiversity intactness of floodplain wetlands. Wetl. Ecol. Manag. 22, 647–658. https://doi.org/10.1007/s11273-014-9360-8.

Lane, C.R., Creed, I.F., Golden, H.E., Leibowitz, S.G., Mushet, D.M., Rains, M.C., Wu, Q., D'Amico, E.D., Alexander, L.C., Ali, G.A., Basu, N.B., Bennett, M.G., Christensen, J. R., Cohen, M.J., Covino, T.P., DeVries, B., Hill, R.A., Jencso, K., Lang, M.W., McLaughlin, D.L., Rosenberry, D.O., Rover, J., Vanderhoof, M.K., 2023. Vulnerable Waters are Essential to Watershed Resilience. Ecosystems 26, 1–28. https://doi.org/10.1007/s10021-021-00737-2.

Luber, H. H. (2002). Floristic Inventory of an Altamaha River Floodplain Area [Master's Thesis, University of Georgia]. https://getd.libs.uga.edu/pdfs/luber_holly_l_200208_ms.pdf.

Morrison, R.R., Simonson, K., McManamay, R.A., Carver, D., 2023. Degradation of floodplain integrity within the contiguous United States. Nature Communications Earth & Environment 4, 215. https://doi.org/10.1038/s43247-023-00877-4.

National Park Service (NPS), 2015. Lowland Forests. Olympic National Park. https://www.nps.gov/olym/learn/nature/lowland-forests.htm.

National Park Service (NPS), 2020. Temperate Rain Forests. Olympic National Park. https://www.nps.gov/olym/learn/nature/temperate-rain-forests.htm.

Nuzzo, R., 2018. Percent Differences: Another Look. *PM&R* 10 (6), 661–664. https://doi.org/10.1016/j.pmrj.2018.05.003.

Oregon State University (OSU). (n.d.). Vascular plant list on the Andrews Experimental Forest and nearby Research Natural Areas, 1958-1979, HJ Andrews Experimental Forest and Long Tern Ecological Research Site. https://andrewsforest.oregonstate.edu/sites/default/files/lter/about/species/HJA_Vascular_Plants_List.pdf.

R Core Team. (2023). R: A language and environment for statistical computing. R Foundation for Statistical Computing. https://www.r-project.org/.

Sabins Jr., F.F., Ellis, J.M., 2020. Remote Sensing: Principles, Interpretation, and Applications, (4th ed.). Waveland Press Inc.

Samaritani, E., Shrestha, J., Fournier, B., Frossard, E., Gillet, F., Guenat, C., Niklaus, P.A., Pasquale, N., Tockner, K., Mitchell, E.A.D., Luster, J., 2011. Heterogeneity of soil carbon pools and fluxes in a channelized and a restored floodplain section (Thur River, Switzerland). Hydrol. Earth Syst. Sci. 15, 1757–1769. https://doi.org/10.5194/hess-15-1757-2011.

Sambrook Smith, G. H., Best, J. L., Bristow, C. S., Petts, G. E., & Jarvis, I. (Eds.). (2006). Braided Rivers: Process, Deposits, Ecology and Management (Special Publication 36 of the IAS). Blackwell Publishing Ltd. https://doi.org/10.1002/9781444304374.

Schindler, S., O'Neill, F.H., Biró, M., Damm, C., Gasso, V., Kanka, R., van der Sluis, T., Krug, A., Lauwaars, S.G., Sebesvari, Z., Pusch, M., Baranovsky, B., Ehlert, T., Neukirchen, B., Martin, J.R., Euller, K., Mauerhofer, V., Wrbka, T., 2016. Multifunctional floodplain management and biodiversity effects: a knowledge synthesis for six European countries. Biodivers. Conserv. 25, 1349–1382. https://doi.org/10.1007/s10531-016-1129-3.

Schumm, S.A., 1985. Patterns of Alluvial Rivers. Annu. Rev. Earth Planet. Sci. 13, 5–27. https://doi.org/10.1146/annurev.ea.13.050185.000253.

Scown, M.W., Thoms, M.C., De Jager, N.R., 2015. Floodplain complexity and surface metrics: Influences of scale and geomorphology. Geomorphology 245, 102–116. https://doi.org/10.1016/j.geomorph.2015.05.024.

Scown, M.W., Thoms, M.C., De Jager, N.R., 2016. An index of floodplain surface complexity. Hydrol. Earth Syst. Sci. 20, 431–441. https://doi.org/10.5194/hess-20-431-2016.

Stoffers, T., Buijse, A.D., Geerling, G.W., Jans, L.H., Schoor, M.M., Poos, J.J., Verreth, J. A.J., Nagelkerke, L.A.J., 2022. Freshwater fish biodiversity restoration in floodplain rivers requires connectivity and habitat heterogeneity at multiple scales. Sci. Total Environ. 838 (Part 4), 156509 https://doi.org/10.1016/j.scitotenv.2022.156509.

Stanford, J. A., Lorang, M. S., & Hauer, F. R. (2005). The shifting habitat mosaic of river ecosystems. *SIL Proceedings, 1922–2010*, *29*(1), 123–136. https://doi.org/10.1080/03680770.2005.11901979.

Open Topography. (2021). *USGS 1/3 arc-second Digital Elevation Model*. https://doi.org/10.5069/G98K778D.

U.S. Environmental Protection Agency (EPA). (2013). *Level III Ecoregions of the Conterminous United States shapefile*. U.S. EPA – National Health and Environmental Effects Research Laboratory. https://www.epa.gov/eco-research/level-iii-and-iv-ecoregions-continental-united-states.

U.S. Geological Survey (USGS). (2016). *McKenzie River Bare Earth Mosaic*. http://prd-tnm.s3.amazonaws.com/index.html?prefix=StagedProducts/Elevation/metadata/OR_McKenzieRiver_2021_B21/OR_McKenzieRiver_1_2021/spatial_metadata/contractor_provided/.

U.S. Geological Survey (USGS). (2018, November 27). *NDVI, the Foundation for Remote Sensing Phenology*. https://www.usgs.gov/special-topics/remote-sensing-phenology/science/ndvi-foundation-remote-sensing-phenology.

U.S. Geological Survey (USGS). (2022a). *Landsat Normalized Difference Vegetation Index*. Landsat Missions. https://www.usgs.gov/landsat-missions/landsat-normalized-difference-vegetation-index.

U.S. Geological Survey (USGS). (2022b). *Normalized Difference Moisture Index*. Landsat Missions. https://www.usgs.gov/landsat-missions/normalized-difference-moisture-index.

U.S. Geological Survey (USGS). (2022c). *StreamStats* (v4.11.1). https://streamstats.usgs.gov/ss/.

U.S. Geological Survey (USGS). (2022d). The National Geologic Map Database MapView. https://ngmdb.usgs.gov/mapview/.

U.S. Geological Survey (USGS). (2023a). *StreamStats* (v4.12.0). https://streamstats.usgs.gov/ss/.

U.S. Geological Survey (USGS). (2023b). *The National Map Download Client* (v2.0). U.S. Geological Survey. https://apps.nationalmap.gov/downloader/.

USDA Natural Resources Conservation Service (NRCS). (2022a). *Olympic National Park Alluvial Units (unofficial/unpublished)*.

USDA Natural Resources Conservation Service (NRCS). (2022b). *Web Soil Survey* (v3.4.0). https://websoilsurvey.sc.egov.usda.gov/App/WebSoilSurvey.aspx.

USDA Natural Resources Conservation Service (NRCS). (2023). *Web Soil Survey*. https://websoilsurvey.sc.egov.usda.gov/App/WebSoilSurvey.aspx.

Wada, T., Chikita, K.A., Kim, Y., Kudo, I., 2011. Glacial Effects on Discharge and Sediment Load in the Subarctic Tanana River Basin, Alaska. Arct. Antarct. Alp. Res. 43 (4), 632–648. https://doi.org/10.1657/1938-4246-43.4.632.

Ward, J.V., Malard, F., Tockner, K., 2002. Landscape ecology: A framework for integrating pattern and process in river corridors. Landsc. Ecol. 17, 35–45. https://doi.org/10.1023/A:1015277626224.

Wohl, E., Iskin, E.P., 2019. Patterns of Floodplain Spatial Heterogeneity in the Southern Rockies, USA. Geophys. Res. Lett. 46 (11), 5864–5870. https://doi.org/10.1029/2019GL083140.

Wohl, E., Marshall, A.E., Scamardo, J., White, D., Morrison, R.R., 2022. Biogeomorphic influences on river corridor resilience to wildfire disturbances in a mountain stream of the Southern Rockies, USA. Sci. Total Environ. 820, 153321 https://doi.org/10.1016/j.scitotenv.2022.153321.